Front dynamics and macroscopic diffusion in buoyant mixing in a tilted tube

T. Séon and J. Znaien
Université Pierre et Marie Curie-Paris 6, Université Paris-Sud, CNRS,
Laboratoire FAST, Bat. 502, Campus Universitaire, Orsay, F-91405, France

B. Perrin
Laboratoire Pierre Aigrain, UMR 8551, CNRS, Ecole Normale Supérieure, Département de Physique,
24 rue Lhomond, 75231 Paris Cedex 05, France

E. J. Hinch
DAMTP-CMS, University of Cambridge, Wilberforce Road, CB3-OWA, Cambridge, United Kingdom

D. Salin and J. P. Hulin
Université Pierre et Marie Curie-Paris 6, Université Paris-Sud, CNRS,
Laboratoire FAST, Bat. 502, Campus Universitaire, Orsay, F-91405, France

The buoyancy driven interpenetration of two fluids of different densities has been studied in a long tilted tube in the strong mixing regime for which the mean concentration profile along the tube length satisfies a macroscopic diffusion equation. Variations of the corresponding macroscopic diffusion coefficient D and of the front velocity V_f are studied as a function of the Atwood number At, the viscosity ν, the tube diameter d, and the tilt angle θ. Introducing the characteristic inertial velocity V_t and the Reynolds number Re_t, the normalized front velocity V_f/V_t and dispersion coefficient $D/(V_t d)$ are observed to scale, respectively, as $\text{Re}_t^{-3/4}$ and $\text{Re}_t^{-3/2}$ for $\text{Re}_t \lesssim 1000$. Also, V_f increases linearly with $\tan\theta$ and the ratio (D/V_f^2) remains of the order of $(35 \pm 10)d/V_t$ in a wide range of values of the tilt angle and of the other control parameters. This close relation observed between the variations of D and V_f^2 is discussed in terms of the characteristic time for transverse mixing across the flow channel. © *2007 American Institute of Physics*. [DOI: 10.1063/1.2821733]

I. INTRODUCTION

Buoyancy induced mixing of liquids is a widespread phenomenon in natural systems (oceanography, hydrology, atmospheric sciences) with large potential consequences on the environment and is also encountered frequently in chemical or petroleum engineering. Such processes are strongly influenced by flow confinement when they take place inside a tilted or vertical tube;[1,2] this is the case for two miscible fluids of different densities suddenly put in contact[3] [the fluids are initially separated in an unstable configuration, each of them occupying half of the tube length as in Fig. 1(a)]. Two types of macroscopic measurements may be performed during the development of mixing between the two fluids:

- The displacement with time of the outer boundaries of the interpenetration zone (this displacement is characterized by a "front velocity" V_f[4]).
- The profile along the tube length of the mean relative concentration $\bar{C}(x,t)$ in the tube section.[5]

For low tilt angles θ of the tube with respect to vertical and high enough relative density contrasts characterized by the Atwood number $\text{At}=(\rho_2-\rho_1)/(\rho_2+\rho_1)$, the profile $\bar{C}(x,t)$ satisfies a diffusion equation $\partial\bar{C}/\partial t=D\partial^2\bar{C}/\partial x^2$ involving a macroscopic diffusion coefficient D.[5] In previous experiments the variations of D and V_f with the tilt angle θ from

vertical have been studied for fluids of different kinematic viscosities ν and displayed similar trends.[4,5]

The present work is therefore devoted to the study of the relation between D and V_f in flow regimes for which both parameters can be measured and of the scaling laws satisfied separately by D and V_f as a function of the experimental parameters.

A possible explanation for the close relation between D and V_f is the fact that the corresponding processes involve the same combination of physical phenomena: the longitudinal interpenetration of the fluids is driven by buoyancy forces proportional to the component of gravity parallel to the tube axis.[6–11] This spreading effect is balanced by transverse mixing in the tube section induced by Kelvin–Helmholtz instabilities of the pseudo-interface between the fluids.[12–14] In tilted tubes, the development of these instabilities is limited by the segregation effect of the transverse gravity component $g\sin\theta$ which acts to keep the two fluids separated.[15,16]

The diffusive spreading of the mean concentration profile is only observed at small tilt angles θ, high density contrasts At, and low viscosities ν; this reflects the fact that an effective transverse mixing is required to achieve this transverse regime. The strong influence of transverse mixing also explains the increase of V_f and D with θ or ν reported in Refs. 4 and 5; mixing becomes poorer, leading to higher local density contrasts and, therefore, to larger local buoy-
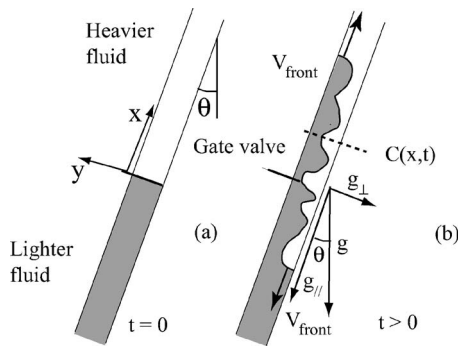
19, 125105-1

FIG. 1. Schematic view of the interpenetration of a light (dark color) and a heavy fluid (light color) inside a tilted tube. (a) Initial configuration with separated fluids. (b) Development of an interpenetration zone after the two fluids have been put in contact.
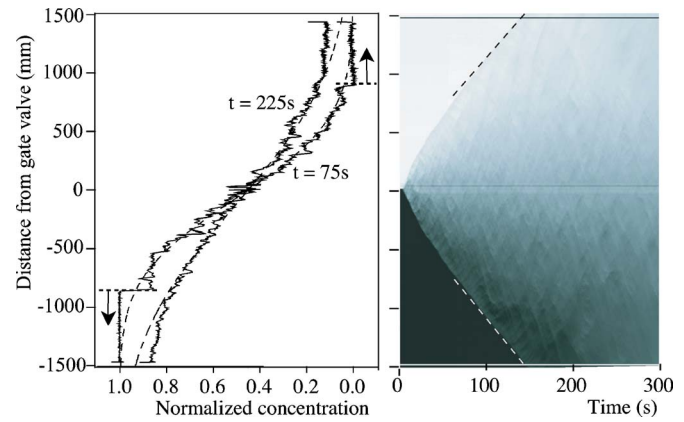

FIG. 2. (Color online) Left—continuous lines: Variation of the mean concentration $\bar{C}(x,t)$ (horizontal scale) with the distance x from the gate valve (vertical scale) at two different times $t=75$ s and $t=225$ s. Dashed lines: Fits of the concentration profiles with solutions of Eq. (1) using the same value of D for the two curves. Dotted lines (respectively, arrows): Location (respectively, direction of motion) of the front at $t=75$ s. Right—spatio-temporal diagram of the variation of the mean concentration $\bar{C}(x,t)$ (gray levels) with the distance x from the gate valve (vertical scale) and time (horizontal scale). θ:30°, At$=4\times10^{-3}$, $\nu=10^{-6}$ m^2 s^{-1}. Dashed lines: Linear fits corresponding to the stationary front velocity.

ancy forces.[17] If θ is increased further with given At and ν values, the spreading of the concentration profile is no longer diffusive and D becomes meaningless. In this domain, the front velocity V_f reaches a value $V_f^M \simeq 0.7(\text{At } gd)^{1/2}$ independent of the viscosity ν; this implies that the front dynamics results solely from a balance between inertial and buoyancy forces with a local density contrast at the front equal to the difference between the densities of the two original fluids (i.e., pure displacing fluid reaches the front[4]). At still higher tilt angles θ (tubes close to horizontal) a viscous counterflow of the two fluids is observed.

In the present work, we study the strong mixing regime in which a macroscopic diffusion coefficient can be measured and all experiments are realized therefore for moderate, although nonzero θ values. The case of vertical tubes has been studied previously and is discussed elsewhere.[3] It has been shown to display special properties compared to the tilted case[5] and, in addition, the velocity V_f is often difficult to determine experimentally when $\theta=0$. The variations of D and V_f with θ and ν, as well as with the tube diameter d and of At will be studied systematically and the corresponding scaling laws as a function of these parameters will be determined. A particularly interesting point will be the proportionality between D and V_f^2 observed in some regimes; their ratio will be related to the characteristic time for transverse mixing across the tube section.

II. EXPERIMENTAL SETUP AND PROCEDURE

The experimental setup has been described in detail in a previous work.[3,5] The experiments use a 4 m long transparent tube which can be tilted at all angles θ from vertical to horizontal. Initially, the lower half of the tube length is filled with a light dyed fluid (salt-nigrosin solution of density ρ_1) while the upper half is filled with a denser transparent fluid (water-CaCl$_2$ solution of density $\rho_2>\rho_1$); the Atwood number At for these pairs of fluids ranged between 4×10^{-4} and 3.5×10^{-2} with a common viscosity $\nu=10^{-6}$ m^2 s^{-1}. In order to investigate the influence of the viscosity, other series of experiments were achieved by adding equal amounts of glycerol to both solutions, leading to $\nu=2\times10^{-6}$, 4×10^{-6}, and 6×10^{-6} m^2 s^{-1}. Most experiments took place inside a tube of diameter $d=20$ mm; other diameter values

$d=30$ mm and $d=12$ mm have also been used in order to analyze the influence of the parameter d. The two fluids are initially separated by a sliding gate valve which is opened at the origin time to start the mixing process. The tube is illuminated from the back and images of the transmitted light are recorded at $0.5-2$ s intervals by a digital camera with a high dynamical range (4096 gray levels). Each image has about 1300×20 pixels. Video recordings of the flow are performed simultaneously; they provide qualitative information at a higher frame rate (25 images per second).

Prior to the experiments, reference images are obtained with the tube fully saturated with transparent and dyed fluid, respectively. After a suitable calibration using images obtained with dye solutions of different concentrations, one obtains maps of the local concentration $\bar{C}(x,y,t)$ (each value corresponds to an integral of the concentration in the third z direction and x is the distance along the tube from the gate valve). In the turbulent mixing regime observed in the present work, the transverse concentration gradients along y are small and almost constant across the tube: one obtains therefore a good estimate of the mean concentration in a section ($x=$cst.) by averaging $\bar{C}(x,y,t)$ over y across the diameter of the tube. Figure 2 (left) displays the profiles along the tube of the normalized concentration $\bar{C}(x,t)$ at two different times.

One observes first that the overall concentration variation has the characteristic error function like shape expected for a diffusive spreading process and that the slope of the profile near the gate valve decreases with time. Also, the location of the fronts at the outer boundaries of the mixing zone is marked on the relative concentration profiles by sharp variations of $\bar{C}(x,t)$ (dotted horizontal lines in the curve $t=75$ s). In order to analyze the motion of these fronts, it is convenient to use spatio-temporal diagrams in which
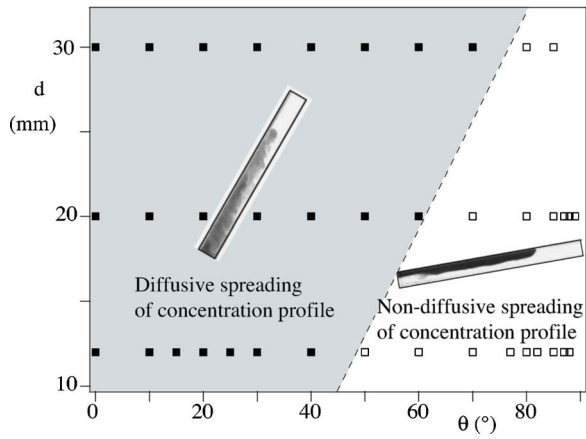
FIG. 3. (Color online) Flow regime map displaying the observation of diffusive (gray shade) regimes in which Eq. (1) is satisfied and nondiffusive ones in tilted tubes. Bottom axis: Tilt angle θ from vertical. Left axis: Tube diameter d. Atwood number At$=10^{-2}$, viscosity $\nu=10^{-6}$ m^2 s^{-1}. Insets: Views of the part of the tube above the gate valve for values of θ and d corresponding approximately to the location of the image on the map.

FIG. 4. Variation of the front velocity V_f as a function of the tilt angle θ for fluids of 3 different viscosities ($\blacksquare$): $\nu=\nu_o=10^{-6}$ m^2 s^{-1}; ($\boxtimes$) $\nu=2\times10^{-6}$ m^2 s^{-1}; ($\boxplus$) $\nu=4\times10^{-6}$ m^2 s^{-1}. Inset: Variation of $V_f/(\nu/\nu_o)^{3/4}$ as a function of θ with the same symbols as in the main graph (At$=10^{-2}$, $d=20$ mm). The dashed line is a guide for the eye.

$\bar{C}(x,t)$ is coded by gray levels in a plane where the coordinates are x and t [Figure 2 (right)]; the locations $X_f(t)$ of the upper and lower front at the different times appear in these diagrams as boundaries between black/light and gray shade regions. The slopes of these boundaries directly provide the front velocities V_f; the velocity values used in the following are determined at times long enough so that a stationary flow regime has been reached and V_f may be considered as constant[17] (dashed line in the figure). The macroscopic diffusion coefficient D is determined by fitting the profiles $\bar{C}(x,t)$ by solutions of the diffusion equation,

$$\frac{\partial\bar{C}}{\partial t}=D\frac{\partial^2\bar{C}}{\partial x^2}. \tag{1}$$

Such fits are shown in Fig. 2 (left) by dashed lines. As observed previously in experiments in vertical[3] and tilted[5] tubes, a good fit is obtained at different times using a single value of the dispersion coefficient D. In all cases, D is many orders of magnitude larger than the molecular diffusion coefficient D_m since the diffusive process reflects random motions of macroscopic fluid packets and not the thermal agitation of molecules. The profiles selected for these fits correspond to times t short enough so that the displacement fronts have not yet reached the ends of the tube and long enough so that the concentration has been homogenized in the tube sections. For each profile, the fits are achieved in the intermediate mixing zone between the fronts where Eq. (1) is satisfied.

The limiting angle θ_c up to which Eq. (1) is valid increases at higher density contrasts and lower viscosities (see Ref. 5). The angle θ_c also increases with the tube diameter d as shown by Fig. 3. The insets of the figure displays views of the flow in the nondiffusive and diffusive regimes; even though segregation effects are visible in both cases, transverse mixing is more efficient in the latter case and homogenizes the concentration in the section after a transition distance from the front, allowing one to observe a diffusive
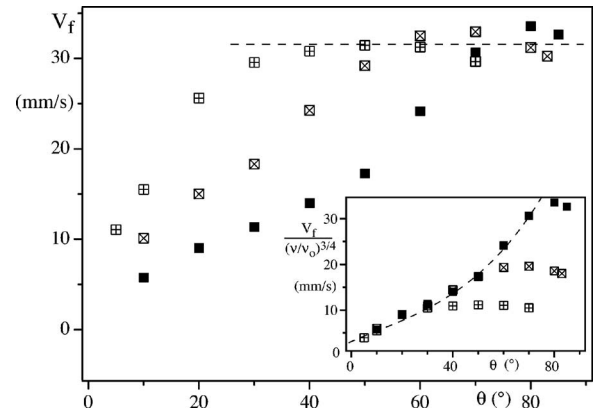
regime for longitudinal spreading. The segregation effects are stronger at higher tilt angles θ, higher viscosities, smaller tube diameters, and lower density contrasts.

Finally we wish to emphasize that, in the diffusive regime, the distance of the isoconcentration points $[\bar{C}(x,t)$ =cst.$]$ of the profile from the gate valve increase as $t^{1/2}$ while the distance $x_f(t)$ of the front from the valve increases as t (in the stationary regime). The front appears therefore as a cutoff point in the concentration profile but, in the same experiment, its motion has advective characteristics while the concentration profile spreads out diffusively.

III. QUANTITATIVE ANALYSIS OF FRONT VELOCITY DEPENDENCE ON EXPERIMENTAL PARAMETERS

A. Front velocity dependence on the fluid viscosity and tube diameter

The front velocity V_f has been measured with fluids of different viscosities[4] ν. For a given angle θ, V_f increases significantly with ν in the strong mixing diffusive regime before reaching the "plateau" value V_f^M independent of ν (Fig. 4). These different data can be collapsed onto the curve corresponding to the lower viscosity $\nu_o=10^{-3}$ m^2 s^{-1} by dividing them by $(\nu/\nu_o)^{3/4}$ (see inset). Several other values of the exponent have been tested indicating an uncertainty of ±0.05 on the value 3/4 of the exponent. In the inset, the data points deviate from the common trend (dashed line) towards the "plateau" value $V_f^M(\nu_o/\nu)^{3/4}$ at a tilt angle θ similar to the upper limit of the diffusive regime (this value of θ decreases, as expected, at higher viscosities).

Another important parameter is the tube diameter. For given values of At, θ, and ν, the front velocity V_f decreases slightly at larger diameters d for low tilt angles, i.e., in the diffusive regime, while the "plateau" value V_f^M increases (Fig. 5). In this case, the variation of V_f with d is too weak and the range of d values is not broad enough to allow one to determine precisely the scaling power law; a value -0.5 ± 0.15 may be estimated for the corresponding exponent. Finally, previous measurements have shown that V_f increased with the Atwood number At, although very slowly.[4]
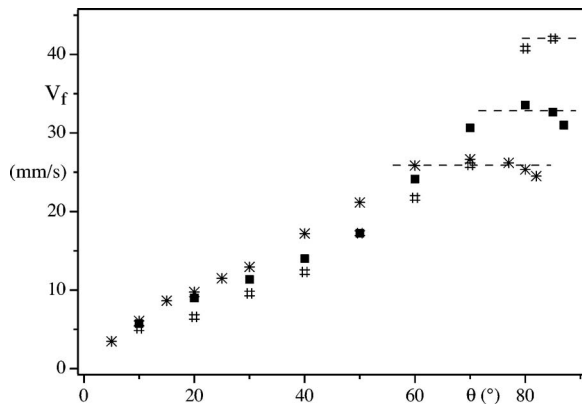
FIG. 5. Variation of the front velocity V_f as a function of the tilt angle θ for 3 different tube diameters: (∗) $d=12$ mm, (■) $d=20$ mm, (#) $d=30$ mm (At$=10^{-2}$, $\nu=10^{-3}$ m^2 s^{-1}).

FIG. 6. Variation of the normalized front velocity $(V_f/V_t)\mathrm{Re}_t^{3/4}$ as a function of $\tan\theta$ for different tube diameters, Atwood numbers and viscosities. The symbols used in the present graph and in Figs. 7–9 correspond to the following parameter values: (●) At$=3.5\times10^{-2}$, (♦) At$=3.9\times10^{-3}$, (▼) At$=1.2\times10^{-3}$, (▲) At$=4\times10^{-4}$, (⊠) $\nu=2\times10^{-6}$ m^2 s^{-1}, (⊞) $\nu=4\times10^{-6}$ m^2 s^{-1}, (∗) $d=12$ mm, (+) $d=12$ mm and At$=2\times10^{-3}$, (×) $d=12$ mm and At$=4\times10^{-2}$, (♯) $d=30$ mm, (⊗) $d=30$ mm and $\nu=2\times10^{-6}$ m^2 s^{-1}, (⊕) $d=30$ mm and $\nu=4\times10^{-6}$ m^2 s^{-1}, (▽) $d=30$ mm and At$=10^{-3}$, and (◇) $d=30$ mm and At$=4\times10^{-3}$; the parameters that are not specifically precise take the values At$=10^{-2}$, $\nu=10^{-6}$ m^2 s^{-1}, $d=20$ mm corresponding to symbol (■). Dashed line: $f(\theta)=12(1+3.6\tan\theta)$.

B. Scaling law for the front velocity in the diffusive regime

We attempt now to account globally for the variations of V_f as a function of d, At, and ν using a single scaling law. The turbulent diffusive mixing regime of interest here is determined by an interplay between buoyancy forces and inertial effects. The logical reference velocity for such flows is therefore the inertial velocity,

$$V_t = \sqrt{\mathrm{At}\, gd}, \tag{2}$$

which physically reflects a balance between buoyancy ($\propto\Delta\rho gd$) and inertial ($\propto\rho V^2$) forces. Within a factor of 0.7, V_t is in addition equal to the front velocity in the weak mixing "plateau" domain.[4] From this characteristic velocity V_t, one defines a characteristic Reynolds number $\mathrm{Re}_t=V_t d/\nu$.

As a first try, we assume that the scaling law satisfied by the front velocity involves only V_t, Re_t, and θ with $V_f/V_t \propto \mathrm{Re}_t^\alpha$. The variation of V_f as $\nu^{3/4}$ determined above requires that $\alpha=-3/4$, leads to the relation

$$\frac{V_f}{V_t} = f(\theta)\mathrm{Re}_t^{-3/4}, \tag{3}$$

which can also be written as

$$V_f = f(\theta)(\mathrm{At}\, g)^{1/8} d^{-5/8} \nu^{3/4}. \tag{4}$$

This relation indeed predicts a very slow increase of V_f with the density contrast (as At$^{1/8}$) and a front velocity decreasing for larger tube diameters as $d^{-5/8}$ in agreement with the previous estimation. As a more quantitative test of this relation, the renormalized ratio $(V_f/V_t)\mathrm{Re}_t^{3/4}$ has been plotted in Fig. 6 as a function of the tangent of the angle θ. A good collapse of all the variations in the diffusive regime is obtained in this way and the common master curve is well fitted by the function $f(\theta)=12(1+3.6\tan\theta)$ (dotted line) as can be seen in Fig. 6. The $\tan\theta$ variation indicates that both the longitudinal and the transverse gravity components influence the mixing process (note that, for values of $\tan\theta$ larger than 1 or so, the difference between θ, $\sin\theta$, and $\tan\theta$ is large enough so that using one parameter instead of one of the others becomes meaningful).
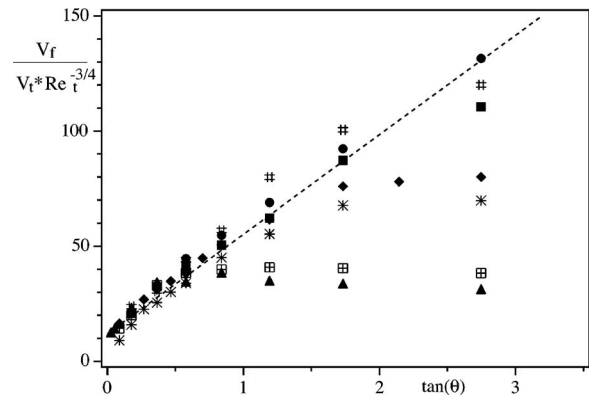
IV. DEPENDENCE OF THE DIFFUSION COEFFICIENT ON THE EXPERIMENTAL PARAMETERS

A. Diffusion coefficient dependence on the Reynolds number

Previous measurements in tilted tubes[5] have shown that, while the macroscopic diffusion coefficient varies very slowly with the Atwood number At, it increases faster with the viscosity, in a manner qualitatively similar to the variation of the front velocity V_f. This suggests an attempt to account for the variations of D by a scaling law of the same type as that used for V_f,

$$\frac{D}{V_t d} = h(\theta)(\mathrm{Re}_t)^{-\beta}, \tag{5}$$

where V_t and d have been selected as the reference parameters for normalizing D. Equivalently, the equation can be rewritten

$$D = h(\theta)(\mathrm{At}\, g)^{(1-\beta)/2} d^{3(1-\beta)/2} \nu^\beta. \tag{6}$$

Attempts to collapse all data on a master curve similar to that of Fig. 6 by plotting $(D/V_t d)(\mathrm{Re}_t)^\alpha$ as a function of θ were however not successful; different values of α were indeed needed to collapse the data points for high and for low values of Re_t. We chose therefore instead to plot in Fig. 7 the variation of the nondimensional macroscopic diffusion coefficient $D/V_t d$ as a function of Re_t for the different values of the tilt angle θ. The sets of points corresponding to the different values of θ are well separated since D significantly increases with θ. In all cases, two domains of variation are observed with a transition at $\mathrm{Re}_t \simeq 1000$. For $\mathrm{Re}_t \lesssim 1000$, $D/(V_t d)$ varies as $\mathrm{Re}_t^{-3/2}$ while, for $\mathrm{Re}_t \gtrsim 1000$, $D/V_t d$ varies slower as $\mathrm{Re}_t^{-1/2}$. These results suggest that the macroscopic diffusion mechanism undergoes a significant change for $\mathrm{Re}_t \simeq 1000$.
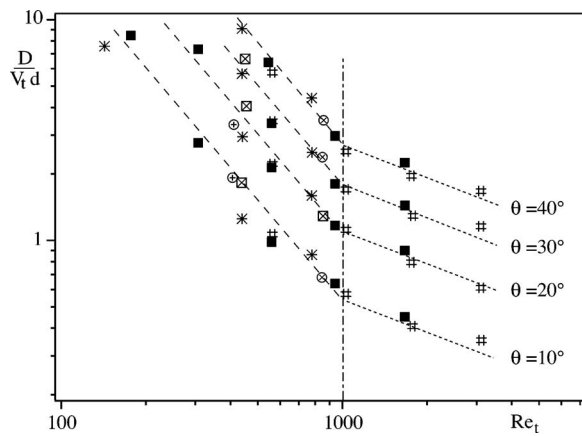
FIG. 7. Variation of the normalized macroscopic diffusion coefficient $D/(V_t d)$ as a function of the Reynolds number $\mathrm{Re}_t = V_t d/\nu$ for different tilt angles $\theta = 10°$, $20°$, $30°$, and $40°$. Slopes of dashed (respectively, dotted) lines $= -3/2$ (respectively, $-1/2$). Vertical dashed-dotted line corresponds to $\mathrm{Re}_t = 1000$. The symbols have the same meaning as in Fig. 6.

B. Scaling properties of the macroscopic diffusion coefficient in the lower Reynolds number regime

In the following, the discussion is focused on the mixing process taking place at $\mathrm{Re}_t \lesssim 1000$ for which a particularly good correlation between D and V_f is observed. In this domain, $\alpha = 3/2$ and one expects D to satisfy the scaling relation derived from Eq. (5),

$$D = h(\theta) V_t d(\mathrm{Re})_t^{-3/2}, \tag{7}$$

or equivalently,

$$D = h(\theta)(\mathrm{At}\, g)^{-1/4} d^{-3/4} \nu^{3/2}. \tag{8}$$

In order to determine the function $h(\theta)$ characterizing the variation of D with the tilt angle, the variation of $D\,\mathrm{Re}_t^{3/2}/(V_t d)$ as a function of θ has been plotted in Fig. 8 (all data points are such that $\mathrm{Re}_t \lesssim 1000$). As could be already expected from Fig. 7 in the range of Re_t values chosen, a very good collapse of all data points onto a same master
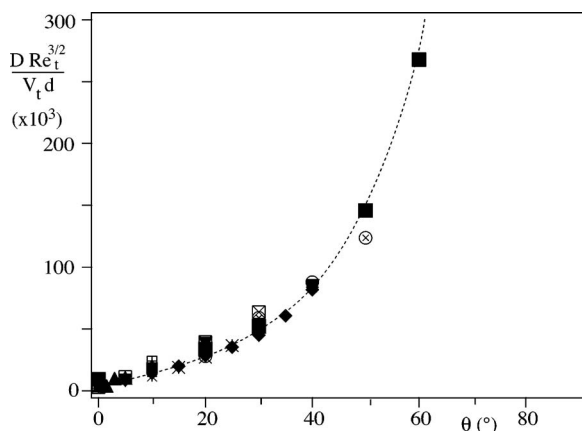

FIG. 8. Variation of the normalized macroscopic diffusion coefficient $D\,\mathrm{Re}_t^{3/2}/(V_t d)$ as a function of the tilt angle θ for different tube diameters, Atwood numbers, and density contrasts. The symbols have the same meaning as in Fig. 6. Dotted line: $h(\theta) = 5 \times 10^3 (1 + 3.6 \tan \theta)^2$.
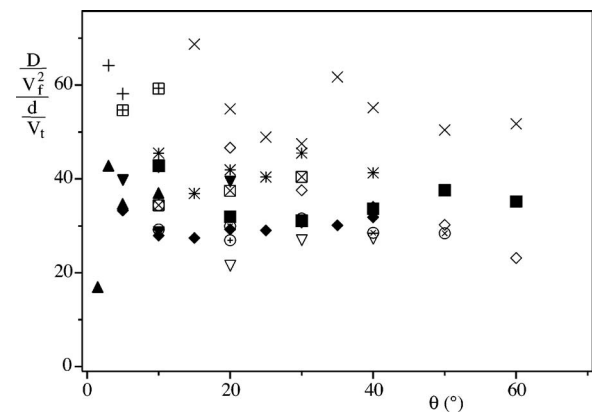

FIG. 9. Variation of the normalized ratio $(D/V_f^2)(V_t/d)$ for $\mathrm{Re}_t < 1000$ as a function of the tilt angle θ for different tube diameters, Atwood numbers, and density contrasts. The symbols have the same meaning as in Fig. 6.

curve is observed. This common trend is observed to be well fitted by the relation $h(\theta) = 5 \times 10^3 (1 + 3.6 \tan \theta)^2$ (dotted line).

V. MACROSCOPIC DIFFUSION COEFFICIENT-FRONT VELOCITY RELATION IN LOWER REYNOLDS NUMBER DOMAIN

Comparing the scaling laws established in the two previous sections for V_f/V_t and $D/(V_f d)$ demonstrates that these dimensionless quantities are extremely closely related. First, they both depend on the variables d, ν, and At only through a power of the dimensionless combination Re_t with an exponent $-3/2$ for D which is twice that for V_f ($-3/4$). Moreover, V_f varies with the tilt angle proportionally to $1 + 3.6 \tan \theta$ while D is proportional to the square of this same expression. Combining these two results, one may infer that the ratio $(D/V_f^2)(d/V_t)$ should depend very little on the experimental parameters.

In order to check this assumption, Fig. 9 displays the variation of $(D/V_f^2)/(d/V_t)$ as a function of θ for different sets of data points corresponding to different values of d, ν, and At. The normalized ratio remains equal to 35 ± 10. This result is verified except for the data points corresponding to $d = 12$ mm and $\mathrm{At} = 4 \times 10^{-2}$ which give 50% higher values. This latter deviation may reflect the fact that the correction introduced by the normalization by d/V_t is found to generally be a little overestimated, particularly for small diameters. As a further check we looked for a possible dependence of the normalized ratio $(D/V_f^2)/(d/V_t)$ on the Reynolds number Re_t. No clear correlation between these quantities was observed. The key point is that the deviations of the values of $(D/V_f^2)/(d/V_t)$ are always small compared to the corresponding variations of the individual values of $(V_f/V_t)^2$ and $D/(V_t d)$ (a factor of more than 1–50).

VI. DISCUSSION OF THE EXPERIMENTAL RESULTS

The results presented above demonstrate that, for values lower than 1000 of the characteristic Reynolds number Re_t, the buoyancy induced mixing flows in tilted tubes display very original and specific features; two very important points

are the simple scaling laws satisfied by the front velocity V_f and macroscopic diffusion coefficient D as a function of the Reynolds number Re_t and the very close relation between these two quantities [more specifically the fact that the dimensionless ratio $(D/V_f^2)/(d/V_t)$ is independent of θ].

A. Interpretation of the ratio D/V_f^2 as a transverse mixing time

In the following, the complicated flow observed in the experiment is modeled as two separate streams of equal cross-sectional area moving up and down at velocities $\pm V$. The average concentrations $C_u(x,t)$ and $C_d(x,t)$ in the areas occupied by the up and down streams vary with the distance x along the tube and in time. We include an exchange transfer between the two streams, proportional to the local difference in concentration, $C_u - C_d$, and with a rate of transfer $1/\tau$. Thus our model is described by the coupled advection-reaction equations,

$$\frac{\partial C_u}{\partial t} + V\frac{\partial C_u}{\partial x} = -\frac{1}{\tau}(C_u - C_d), \qquad (9)$$

$$\frac{\partial C_d}{\partial t} - V\frac{\partial C_d}{\partial x} = +\frac{1}{\tau}(C_u - C_d). \qquad (10)$$

We assume that the velocity V and rate of transfer $1/\tau$ are constants and do not vary in time or position along the tube. We consider the mean concentration given by $\bar{C} = \frac{1}{2}(C_u + C_d)$. By adding and subtracting the pair of equations, we obtain a single second-order equation for $\bar{C}$,

$$\frac{\tau}{2}\frac{\partial^2 \bar{C}}{\partial t^2} + \frac{\partial \bar{C}}{\partial t} = \frac{V^2\tau}{2}\frac{\partial^2 \bar{C}}{\partial x^2}. \qquad (11)$$

This is the classical telegraph equation[18] to be solved subject to the initial condition of a step change,

$$\bar{C} = \begin{cases} 1 & x < 0, \\ 0 & x > 0. \end{cases}$$

The problem can be solved by Fourier transforms. The solution has fronts propagating at velocities $\pm V$, with no change from the initial values ahead of the fronts. The jump in concentration across the fronts decays in time as $\pm\frac{1}{2}e^{-t/\tau}$. In the central section away from the fronts, the solution changes relatively slowly, so that the second derivative in time becomes negligible, leaving the behavior governed by a diffusion equation with an effective diffusivity,

$$D = \frac{1}{2}V^2\tau.$$

This simple model shows that the ratio D/V^2 is constant as a result of the constant exchange rate $1/\tau$ between the two streams. Such a result has some analogy with Taylor dispersion in a laminar flow inside a capillary tube of radius a, where transverse molecular diffusion across the tube section occurs on a time scale $\tau_D = a^2/D_m$, resulting in longitudinal dispersion of coefficient $D \sim U^2 a^2/D_m = U^2\tau_D$.[19,20]

While this simple model helps understand the relation between the diffusive behavior and the propagating fronts with $D/V^2 = \tau/2$, it is not complete. Indeed, the model does

not propose values of the parameters V and τ. Hence it cannot offer any insight into why the value of τ seems to vary little with the angle θ and other variables in the experiment.

A more significant shortcoming is the detail that the jump in concentration at the front decreases exponentially in time, while in Ref. 17 we found it decreased in time to a nonzero constant value. However, the model does not attempt to include any additional physics of the front.

B. Characteristic transverse mixing times

As an example, for a typical Atwood number $At = 4 \times 10^{-3}$ and a tube of diameter $d = 20$ mm, the ratio d/V_t is of the order of 0.7 s, leading to $D/V_f^2 \simeq 25$ s using the mean value 35 of the data points in Fig. 9. Since d/V_t does not depend on θ or ν, the weak variations of $(D/V^2)/(d/V_t)$ imply that the mixing time τ is nearly independent both of θ and ν. This constant value of τ contrasts with the variability of the qualitative and visual properties of the corresponding flows; it implies that the fast increase of D with θ reflects the variation of the front velocity V_f and not that of the exchange time.

More precisely, transverse mixing is directly related to the development of Kelvin–Helmholtz instabilities and their development should depend both on the viscosity (due to viscous damping) and on the tilt angle (due to segregation effects). Regarding the influence of viscosity and following Ref. 21, the growth rate should reflect the viscous diffusion time $\tau_d = d^2/\nu$ at low values of the Reynolds number Re_t and the convective time $\tau_c = d/V_f$ at higher ones. This would suggest using $\tau_d = d^2/\nu$ rather than d/V_t as the characteristic normalization time for the ratio D/V_f^2 at low Reynolds numbers $Re_t < 1000$. The collapse of the data points is found instead to be poorer when this normalization is applied in Fig. 9. This implies that other mechanisms are also active in this range of Re_t values; the influence of the segregation effects should for instance be taken into account.

Some of these flows display intermittency which provides a direct physical meaning to the time τ. In this case, one observes during a fraction of the time a stable counterflow of the heavier and lighter fluids at velocities increasing with time until Kelvin–Helmholtz instabilities develop and trigger an intense mixing between the fluids while strongly reducing the counterflow. Then the instabilities damp out, the counterflow appears and another cycle begins. In this intermittent regime, the characteristic time of transverse mixing is of the order of the period of the intermittency: In several experiments it has been found to be of the same order of magnitude (20–30 s) as the values quoted above for τ_d. This latter point is now being investigated experimentally.

Note finally that, when the diffusive spreading process is considered as a random walk, the duration of the steps is of the order of τ (independent of θ and ν) and their characteristic length is of the order of $V_f\tau$. The length of the steps increases therefore strongly both with θ and the viscosity ν until the number of steps in the length of the tube is not large enough and the conditions for applying the central limit theorem are not satisfied; then, the spreading of the concentration profile is no longer diffusive.

VII. CONCLUSION

The present experimental work has demonstrated that, for inertial Reynolds numbers Re_t below 1000, there is a close relation between the front velocity V_f and the macroscopic diffusion coefficient D describing the spreading of the concentration profile. Both quantities satisfy simple scaling laws as a function of Re_t and θ and the ratio D/V_f^2 can be interpreted as a transverse exchange time τ. Moreover, in contrast to D and V_f, the normalized time $\tau/(d/V_t)$ does not display any coherent variation trend with θ. Overall, its variations are much smaller (typically $\pm30\%$) than those of the dispersion coefficient or of the square of the front velocity taken separately. This transverse exchange time appears therefore as a key parameter of the phenomenon. Another important feature is the transition towards a slower variation of $D/(V_t d)$ as $Re_t^{-1/2}$ (instead of $Re_t^{-3/2}$) for $Re_t > 1000$. This implies that the mechanism for transverse mixing is different in this range of high Re_t values.

A detailed analysis of the dynamics of the mixing process at the local scale is needed to account further for these results and model in particular the dynamics of transverse mixing and its dependence on the experimental parameters.

[1] E. E. Zukoski, "A review of flows driven by natural convection in adiabatic shafts," NIST Report No. NIST-GCR-95-679 (1995), and references therein; J. B. Cannon and E. E. Zukoski, "Turbulent mixing in vertical shafts under conditions applicable to fires in high rise buildings," Technical Fire Report No. 1 to the National Science Foundation, California Institute of Technology, Pasadena, California (1975).

[2] M. H. I. Baird, K. Aravamudan, N. V. Rama Rao, J. Chadam, and A. P. Peirce, "Unsteady axial mixing by natural convection in a vertical column," AIChE J. **38**, 1825 (1992).

[3] M. Debacq, V. Fanguet, J. P. Hulin, D. Salin, and B. Perrin, "Self-similar concentration profiles in buoyant mixing of miscible fluids in a vertical tube," Phys. Fluids **13**, 3097 (2001).

[4] T. Séon, D. Salin, J. P. Hulin, B. Perrin, and E. J. Hinch, "Buoyancy driven front dynamics in tilted tubes," Phys. Fluids **17**, 031702 (2005).

[5] T. Séon, J. P. Hulin, D. Salin, B. Perrin, and E. J. Hinch, "Buoyant mixing of miscible fluids in tilted tubes," Phys. Fluids **16**, L103 (2004).

[6] D. H. Sharp, "An overview of Rayleigh–Taylor instability," Physica D **12**, 3 (1984).

[7] G. K. Batchelor and J. M. Nitsche, "Instability of stationary unbounded stratified fluid," J. Fluid Mech. **227**, 357 (1991); "Instability of stratified fluid in a vertical cylinder," *ibid.* **227**, 419 (1991).

[8] P. E. Linden, J.-M. Redondo, and D. L. Young, "Molecular mixing in the Rayleigh–Taylor instability," J. Fluid Mech. **265**, 27 (1994).

[9] S. B. Dalziel, P. F. Linden, and D. L. Young, "Self-similarity and internal structure of turbulence induced by Rayleigh–Taylor instability," J. Fluid Mech. **399**, 1 (1999).

[10] A. W. Cook and P. E. Dimotakis, "Transition stages of Rayleigh–Taylor instability between miscible fluids," J. Fluid Mech. **443**, 69 (2001).

[11] J. Fernandez, P. Kurowski, P. Petitjeans, and E. Meiburg, "Density driven, unstable flows of miscible fluids in a Hele-Shaw cell," J. Fluid Mech. **451**, 239 (2002).

[12] T. H. Ellison and J. S. Turner, "Turbulent entrainment in stratified flows," J. Fluid Mech. **6**, 423 (1959).

[13] S. A. Thorpe, "Experiments on the instability of stratified shear flows: Miscible fluids," J. Fluid Mech. **46**, 299 (1971).

[14] O. Pouliquen, J. M. Chomaz, and P. Huerre, "Propagating Holmboe waves at the interface between two immiscible fluids," J. Fluid Mech. **266**, 277 (1994).

[15] G. A. Lawrence, F. K. Browand, and L. G. Redekopp, "The stability of the sheared density interface," Phys. Fluids A **3**, 2360 (1991).

[16] E. J. Strang and H. J. S. Fernando, "Entrainment and mixing in stratified shear flows," J. Fluid Mech. **428**, 349 (2001).

[17] T. Séon, J. P. Hulin, D. Salin, B. Perrin, and E. J. Hinch, "LIF measurements of buoyancy driven mixing in tilted tubes," Phys. Fluids **18**, 041701 (2006).

[18] S. Goldstein, "On diffusion by discontinuous movements and on the telegraph equation," Q. J. Mech. Appl. Math. **4**, 129 (1951).

[19] G. I. Taylor, "Dispersion of soluble matter in solvent flowing slowly through a tube," Proc. R. Soc. London, Ser. A **219**, 186 (1953).

[20] R. Aris, "On the dispersion of a solute in a fluid flowing through a tube," Proc. R. Soc. London, Ser. A **253**, 67 (1956).

[21] E. Villermaux, "On the role of viscosity in shear instabilities," Phys. Fluids **10**, 368 (1998).